Table VIII. Gross Mulliken Atomic Charges in $XYOs_3(CO)_{10}$ Clusters

XY	gross atomic charges			
	Os[a]	Os*[b]	X	H
HCl	0.303+	0.191-	0.345-	0.422-
HBr	0.287+	0.192-	0.296-	0.424-
HI	0.276+	0.194-	0.252-	0.427-
Cl_2	0.233+	0.237-	0.328-	
Br_2	0.210+	0.243-	0.328-	
I_2	0.190+	0.248-	0.252-	

[a] Os represents one of the two Os's in the $Os(CO)_3$ fragments. [b] Os* represents the Os in the $Os(CO)_4$ fragment.

interaction is through the e_g-like and 13a' orbitals. Table VIII shows the Mulliken atomic charges, which show a definite shift of electron density from the two bridged Os atoms to Os* and the bridging atoms.

$(\mu$-Cl)$_2$Os$_3$(CO)$_{10}$. The overlap populations in Table VII indicate that the Os–Os* bond is equivalent in strength to the Os–Os* bond in the HX derivatives. The Os–Os overlap population suggests no direct M–M bonding between the two $Os(CO)_3$ fragments. The $Os(CO)_3$ fragments' diffuse 13a' orbitals have a negative overlap population, and this may contribute to an overall Os–Os antibonding interaction. As expected, the overlap populations for X_2 (X = Cl, Br, I) when bonded to the triosmium decacarbonyl moiety were found to be essentially zero. The donation of Os electron density to the antibonding LUMO of X_2 eliminates the bonding in the X_2 molecule.

The Mulliken atomic charges, shown in Table VIII, indicate the shift of electron density from the $Os(CO)_3$ fragments to the bridging halogens. The Os* atoms become more negative as the halogens change from Cl to Br to I. Our calculations suggest that the halogens interact with the Os* indirectly through the bridging Os. This interaction was also hinted by the destabilization of the t_{2g}-like peaks in the PE spectra.

Conclusion

The PE spectra and MO calculations suggest that the only direct Os–Os bonds in both of these bridging series are the two $(CO)_4Os$–$Os(CO)_3$ bonds. The $(CO)_3Os$–$Os(CO)_3$ interaction in the $(\mu$-H)$(\mu$-X) series is weakly bonding due to the diffuse 13a' interactions, while that in the $(\mu$-X$)_2$ series is weakly antibonding. The MO calculations suggest that the t_{2g}-like $Os(CO)_3$ orbitals, which are usually considered only M–CO π bonding, interact strongly with the bridging H and halogen atoms. Changes in the PE spectra are observed as a result of this interaction.

Acknowledgment is made to the Robert A. Welch Foundation (Grant A-648) and the National Science Foundation (Grant CHE 79-20993) for support of this work.

Registry No. 1, 12557-93-6; (μ-H)(μ-Br)$Os_3(CO)$, 61199-98-2; (μ-H)(μ-I)$Os_3(CO)_{10}$, 61199-99-3; (μ-Cl)$_2Os_3(CO)_{10}$, 28109-18-4; (μ-Br)$_2Os_3(CO)_{10}$, 28109-19-5; (μ-I)$_2Os_3(CO)_{10}$, 87101-94-8.

Contribution from the Istituto FRAE-CNR, Bologna, Italy, Istituto Chimico "G. Ciamician", University of Bologna, Bologna, Italy, and Institute of Inorganic Chemistry, University of Fribourg, Fribourg, Switzerland

Excited-State Properties of Complexes of the Ru(diimine)$_3^{2+}$ Family

FRANCESCO BARIGELLETTI,[1] ALBERTO JURIS,[1,2] VINCENZO BALZANI,*[1,2] PETER BELSER,[3] and ALEX VON ZELEWSKY*[3]

Received February 15, 1983

The absorption spectra, emission spectra, emission lifetimes, and temperature dependence of emission intensity and lifetime (between 84 and 330 K) of the complexes $Ru(bpy)_3^{2+}$, $Ru(bpy)_2(biq)^{2+}$, and $Ru(biq)_3^{2+}$ are reported (bpy = 2,2'-bipyridine, biq = 2,2'-biquinoline). The $Ru(biq)_3^{2+}$ complex exhibits metal-to-ligand charge-transfer absorption and emission bands red shifted by about 3000 cm^{-1} compared with the corresponding bands of $Ru(bpy)_3^{2+}$. In the mixed-ligand complex, distinct Ru → bpy and Ru → biq charge-transfer absorptions are present, but emission only occurs from the lowest excited state, which is a Ru → biq charge-transfer state. The temperature dependence of the luminescence emission indicates that in $Ru(biq)_3^{2+}$ a short-lived excited state (most likely a triplet metal-centered state) lies 2700 cm^{-1} above the emitting charge-transfer level. In $Ru(bpy)_2(biq)^{2+}$, there are two low-lying Ru → biq charge-transfer excited states separated by 400 cm^{-1} which presumably originate from the splitting of the metal t_{2g} orbitals in the reduced C_{2v} symmetry of the complex, while the lowest triplet metal-centered excited state lies more than 5500 cm^{-1} above. The photochemical implications of these results are briefly discussed.

Introduction

Complexes of the Ru(diimine)$_3^{2+}$ family, particularly Ru(bpy)$_3^{2+}$, have recently been the object of much interest because of their unique excited-state properties[4-7] and of their use as photosensitizers in the photochemical conversion of solar energy.[7-12] There has also been some controversy concerning the exact nature of the emitting excited state and of the other excited states which are of importance for the photochemical and photophysical properties.[4,6,13-17] In an attempt to understand the details of the electronic states of such complexes and with the aim of tuning their properties in a controlled manner, we have synthesized[18] a series of Ru(II) complexes with ligands of different size and different electronic structure

(1) Istituto FRAE-CNR.
(2) University of Bologna.
(3) University of Fribourg.
(4) Crosby, G. A. *Acc. Chem. Res.* **1975**, *8*, 231.
(5) Kemp, T. J. *Prog. React. Kinet.* **1980**, *10*, 301.
(6) DeArmond, M. K.; Carlin, C. M. *Coord. Chem. Rev.* **1981**, *36*, 325.
(7) Kalyanasundaram, K. *Coord. Chem. Rev.* **1982**, *46*, 159.
(8) Meyer, T. J. *Isr. J. Chem.* **1977**, *15*, 200.
(9) Balzani, V.; Bolletta, F.; Gandolfi, M. T.; Maestri, M. *Top. Curr. Chem.* **1978**, *75*, 1.
(10) Sutin, N.; Creutz, C. *Pure Appl. Chem.* **1980**, *52*, 2717.
(11) Whitten, D. G. *Acc. Chem. Res.* **1980**, *13*, 83.
(12) Graetzel, M. *Acc. Chem. Res.* **1981**, *14*, 376.
(13) Hager, G. D.; Crosby, G. A. *J. Am. Chem. Soc.* **1975**, *97*, 7031. Hager, G. D.; Watts, R. J.; Crosby, G. A. *Ibid.* **1975**, *97*, 7037.
(14) Felix, F.; Ferguson, J.; Güdel, H. U.; Ludi, A. *Chem. Phys. Lett.* **1979**, *62*, 153. Felix, F.; Ferguson, J.; Güdel, H. U.; Ludi, A. *J. Am. Chem. Soc.* **1980**, *102*, 4096. Ferguson, J.; Herren, F. *Chem. Phys. Lett.* **1982**, *89*, 371. Ferguson, J.; Krausz, E. R. *Ibid.* **1982**, *93*, 21.
(15) Vanquickenborne, L. G.; Ceulemans, A. *Inorg. Chem.* **1978**, *17*, 2730. Ceulemans, A.; Vanquickenborne, L. G. *J. Am. Chem. Soc.* **1981**, *103*, 2238.
(16) Belser, P.; Daul, C.; von Zelewsky, A. *Chem. Phys. Lett.* **1981**, *79*, 596.
(17) Kober, E. M.; Meyer, T. J. *Inorg. Chem.* **1982**, *21*, 3967.
(18) Belser, P.; von Zelewsky, A. *Helv. Chim. Acta* **1980**, *63*, 1675.

0020-1669/83/1322-3335$01.50/0

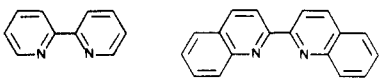

bpy biq

Figure 1. Structural formulas of 2,2′-bipyridine (bpy) and 2,2′-biquinoline (biq).

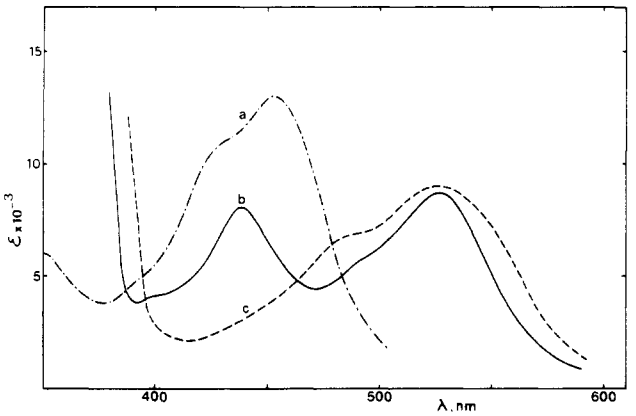

Figure 2. Absorption spectra in alcoholic solution at room temperature of (a) $Ru(bpy)_3^{2+}$, (b) $Ru(bpy)_2(biq)^{2+}$, and (c) $Ru(biq)_3^{2+}$.

and we have studied their electrochemical[18] and photophysical[19-22] properties.

In this paper we report the results of an investigation on the temperature dependence (between 84 and 330 K) of the luminescence emission of the $Ru(bpy)_2(biq)^{2+}$ and $Ru(biq)_3^{2+}$ complexes, where bpy = 2,2′-bipyridine and biq = 2,2′-biquinoline (Figure 1). Absorption spectra, emission spectra, and emission lifetimes at 77 and 293 K were previously reported when we discussed the possibility of using these complexes as photosensitizers for the water-splitting reaction.[20,23] For the sake of comparison, the present temperature dependence investigation has been extended to the already studied[5,13,24-26] $Ru(bpy)_3^{2+}$ complex. A comparative discussion of the results obtained is presented, and it is shown that the behavior of the three complexes can be rationalized on the basis of states derived from a simple orbital model.

Experimental Section

The preparation of $Ru(bpy)_3^{2+}$, $Ru(bpy)_2(biq)^{2+}$, and $Ru(biq)_3^{2+}$ has been reported elsewhere.[18] Diluted solutions (10^{-5}–10^{-4} M) of each complex in ethanol–methanol (4:1 v/v) or propionitrile–butyronitrile (0.71:0.89 v/v) were sealed under vacuum in 1-cm quartz cells after repeated freeze–pump–thaw cycles. The absorption spectra were recorded with a Perkin-Elmer 323 spectrophotometer. The emission spectra (84–330 K) were obtained with a Perkin-Elmer MPF-44B spectrofluorimeter. Excitation was performed in the high-intensity bands of the visible region or at 337 nm, with the same results. The relative emission intensities at the various temperatures were obtained from the area of the emission bands.

Emission lifetimes were measured by a modified Applied Photophysics single photon counting apparatus equipped with a nitrogen thyratron gated source lamp. The decay was monitored at the maximum of the emission band. Data treatment was carried out with a PDP/11 microcomputer. Standard iterative nonlinear programs[27] were employed to analyze the emission curves. The quality of the fit was assessed by the χ^2 values close to unity and the residuals regularly distributed along the time axis. Single exponential decays were observed for each complex in all cases.

For temperature-dependence experiments, the samples were maintained inside a Thor C600 nitrogen-flow cryostat, equipped with a Thor 3030 temperature controlled and indicator. The absolute error is estimated to be ±2 K.

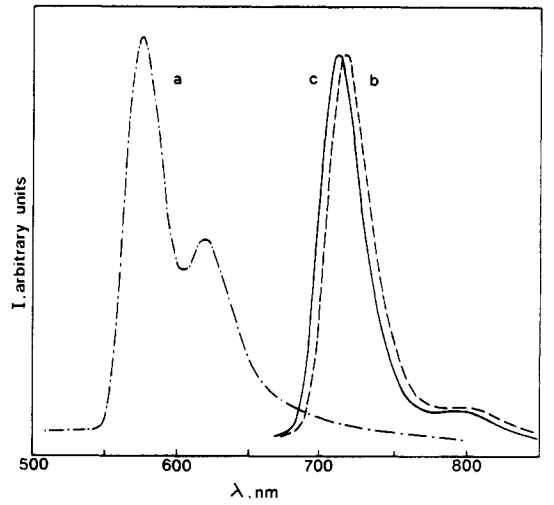

Figure 3. Emission spectra in alcoholic solution at 84 K of (a) $Ru(bpy)_3^{2+}$, (b) $Ru(bpy)_2(biq)^{2+}$, and (c) $Ru(biq)_3^{2+}$.

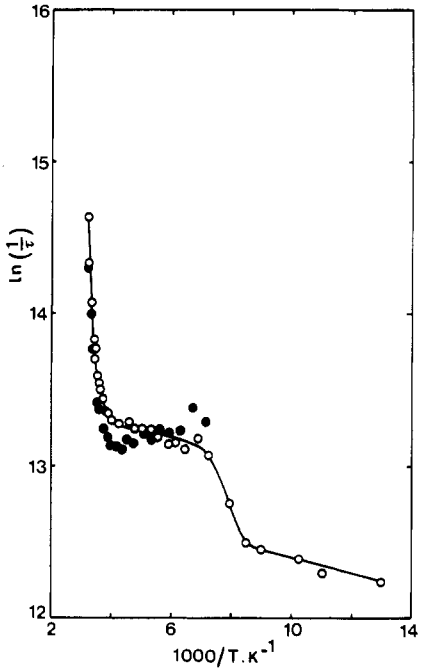

Figure 4. Temperature dependence of emission lifetime (○) and relative emission intensity (●) in alcoholic solution for $Ru(bpy)_3^{2+}$.

Results

The absorption spectra of $Ru(bpy)_3^{2+}$, $Ru(bpy)_2(biq)^{2+}$, and $Ru(biq)_3^{2+}$ in ethanol–methanol at room temperature are shown in Figure 2, and the emission spectra in the same solvent at 84 K are shown in Figure 3.

Figures 4–6 show the temperature dependence of emission lifetimes and relative emission intensities as $\ln(1/\phi_e) + c$ (where c is an arbitrary scaling constant) for the three complexes. In these figures the experimental points are fitted by

(19) Juris, A.; Balzani, V.; Belser, P.; von Zelewsky, A. *Helv. Chim. Acta* **1981**, *64*, 2175.
(20) Juris, A.; Barigelletti, F.; Balzani, V.; Belser, P.; von Zelewsky, A. *Isr. J. Chem.* **1982**, *22*, 87.
(21) Belser, P.; von Zelewsky, A.; Juris, A.; Barigelletti, F.; Tucci, A.; Balzani, V. *Chem. Phys. Lett.* **1982**, *89*, 101.
(22) Belser, P.; von Zelewsky, A.; Juris, A.; Barigelletti, F.; Balzani, V., submitted for publication in *Gazz. Chim. Ital.*
(23) Similar results have been more recently reported: Klassen, D. M. *Chem. Phys. Lett.* **1982**, *93*, 383.
(24) Van Houten, J.; Watts, R. J. *J. Am. Chem. Soc.* **1976**, *98*, 4853.
(25) Durham, B.; Caspar, J. V.; Nagle, J. K.; Meyer, T. J. *J. Am. Chem. Soc.* **1982**, *104*, 4803.
(26) Allsopp, S. R.; Cox, A.; Kemp, T. J.; Reed, W. J. *J. Chem. Soc., Faraday Trans. 1* **1978**, *74*, 1275.
(27) Bevington, P. R. "Data Reduction and Error Analysis for Physical Sciences"; McGraw-Hill: New York, 1969.

Table I. Kinetic Data for Excited-State Decay Obtained by Temperature-Dependent Lifetime Measurements

complex		k_0, s^{-1}	A_1, s^{-1}	ΔE_1, cm^{-1}	A_2, s^{-1}	ΔE_2, cm^{-1}
Ru(bpy)$_3^{2+}$ [a]	I[c]	3.2×10^5	1.4×10^{14}	3950	4.6×10^5	84
	II[d]	2.2×10^5	2.0×10^{14}	4040	5.0×10^5	69
Ru(bpy)$_2$(biq)$^{2+}$ [a]	I	1.4×10^6	2.0×10^7	420		
	II	1.4×10^6	2.0×10^7	410		
Ru(biq)$_3^{2+}$ [b]	I	4.5×10^5	1.8×10^{13}	2700		
	II	4.5×10^5	1.7×10^{13}	2690		

[a] Alcoholic solution. [b] Nitrile solution. [c] Full temperature range (eq 1 and 2, see text). [d] Fluid solution (eq 1, see text).

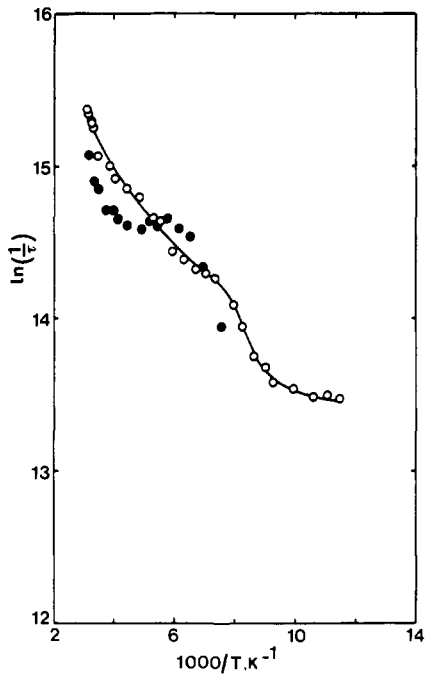

Figure 5. Temperature dependence of emission lifetime (O) and relative emission intensity (●) in alcoholic solution for Ru(bpy)$_2$(biq)$^{2+}$.

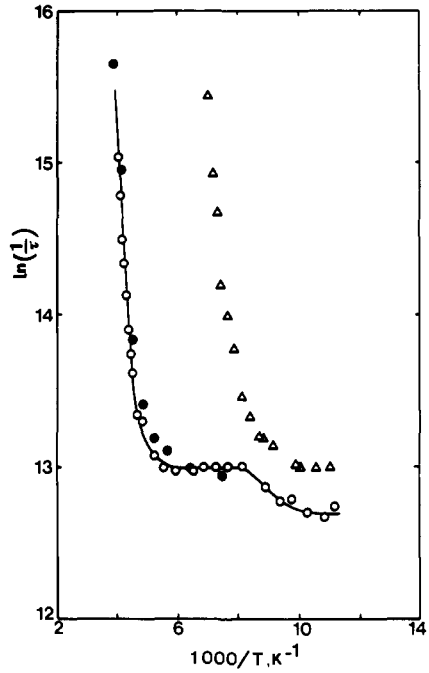

Figure 6. Temperature dependence of emission lifetime (O) and relative emission intensity (●) in nitrile solution and emission lifetime (△) in alcoholic solution for Ru(biq)$_3^{2+}$.

a nonlinear procedure; plots are displayed on a semilogarithmic scale. Emission intensities are reported only for $T > T_g$, where T_g is the temperature corresponding to the melting region of the solvent. As one can see from Figures 4–6, a strong discontinuity was observed for ln $(1/\tau)$ vs. $1/T$ around T_g (see also ref 5). In methanol–ethanol, most of the ln $(1/\tau)$ vs. $1/T$ curve for Ru(biq)$_3^{2+}$ falls in this critical region. Thus, the behavior of this complex was also examined in the propionitrile–butyronitrile solvent, which has a lower melting temperature.

The experimental values of ln $(1/\tau)$ vs. $1/T$ above the melting temperature were fitted by the expression[5]

$$1/\tau = k_0 + A_1 e^{-\Delta E_1/RT} + A_2 e^{-\Delta E_2/RT} \quad (1)$$

For the fitting on the overall temperature range explored, the same expression was used with

$$k_0 = k'_0 + B/\{1 + \exp[C(1/T - 1/T_g)]\} \quad (2)$$

where k'_0 is the temperature-independent term in the glass and the second term on the right-hand side takes care empirically of the fluid–glass transition. The values of the various parameters extracted from the fitting procedure are reported in Table I.

Discussion

Absorption Spectra. It is well-known[4-7] that the high-intensity absorption band of Ru(bpy)$_3^{2+}$ with a maximum at 452 nm (Figure 2) is due to metal-to-ligand charge-transfer (MLCT) transitions. There is now a general agreement[14-16] that the two intense components of the MLCT absorption correspond to $a_2(\pi^*)$ and $e(\pi^*)$ interligand orbitals derived from ψ^* ligand orbitals, antisymmetric with respect to the twofold ligand axis.[15] This is in agreement with MO calculations of EH type which show an energy separation of 1.0 eV between the ψ and χ orbitals of the free bpy ligand, while the calculated separation is only 0.3 eV for phenanthroline, where the $\psi + \chi$ hypothesis for π-acceptor orbitals seems appropriate.[15] For Ru(biq)$_3^{2+}$, the absorption spectrum (Figure 2) shows a band that is quite similar in shape to that of Ru(bpy)$_3^{2+}$ but is red shifted by about 3000 cm^{-1}. This shift is due to the lower energy of the π^*-acceptor orbitals in biq, as is shown by the less negative reduction potentials of biq compared with those of bpy ($\Delta V = 0.47$ V) and of Ru(biq)$_3^{2+}$ compared with Ru(bpy)$_3^{2+}$ ($\Delta V = 0.45$ V).[21] The calculated separation between ψ and χ type orbitals of biq is 1.1 eV, and the absorption band of Ru(biq)$_3^{2+}$ can be assigned within the "ψ-only" model as in the case of Ru(bpy)$_3^{2+}$. The mixed-ligand complex Ru(bpy)$_2$(biq)$^{2+}$ shows two distinct MLCT absorption bands (Figure 2),[20,23] one at 439 nm corresponding to the Ru(bpy)$_3^{2+}$ absorption and the other at 525 nm corresponding to the Ru(biq)$_3^{2+}$ band. This behavior indicates that the two bands of Ru(bpy)$_2$(biq)$^{2+}$ are due to Ru → bpy and Ru → biq transitions and shows that the energies of the ligand π^* orbitals are little influenced by ligand–ligand interactions. The relatively low intensity of the CT band in the (biq)$_3$ complex compared with the analogous band of the Ru(bpy)$_3^{2+}$ complex is presumably due to a smaller metal–ligand orbital overlap caused by steric hindrance.

Emission Spectra. The well-known emission band of Ru(bpy)$_3^{2+}$ at 582 nm (Figure 3), which is due to the lowest ^{3}MLCT excited state,[28] is red shifted by 3200 cm^{-1} in the

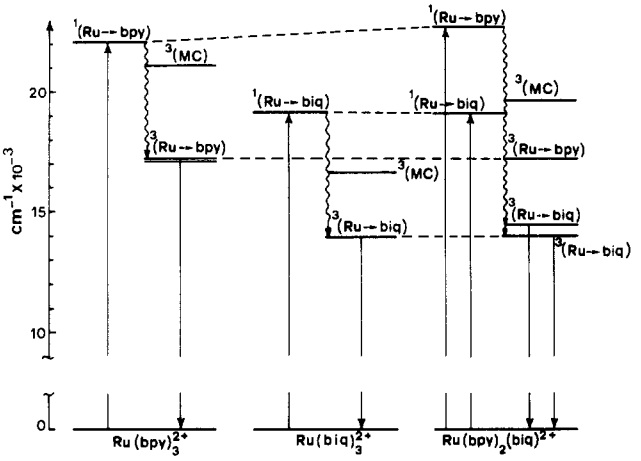

Figure 7. Schematic energy level diagram for $Ru(bpy)_3^{2+}$, $Ru(biq)_3^{2+}$, and $Ru(bpy)_2(biq)^{2+}$.

$Ru(biq)_3^{2+}$ complex (λ_{max} = 718 nm). This shift is comparable with that exhibited by the reduction potential and by the maximum of the absorption band, showing that emission originates from a ^{3}MLCT excited state also in the case of $Ru(biq)_3^{2+}$. The shape of the emission band and the emission lifetime (2.6 μs at 77 K) confirm this assignment.

The emission spectrum of the mixed-ligand complex shows only one emission band, quite similar in energy (λ_{max} = 728 nm) and shape to the band of $Ru(biq)_3^{2+}$ (Figure 3). No emission is observed in the 600-nm region. These results are obtained regardless of whether excitation is performed in the 450- or 520-nm absorption band. This behavior shows that (i) emission only occurs from the lowest excited state of the complex, which is a Ru → biq CT state, and (ii) efficient conversion of Ru → bpy excited states to the lowest Ru → biq excited state takes place. These results are similar to those obtained for the $Ru(phen)_n(biq)_{3-n}^{2+}$[23] and $Ru(bpy)_n(pq)_{3-n}^{2+}$[29] (pq = 2-(2-pyridyl)quinoline) complexes, while for the complexes of the analogous $Ru(phen)_n(pq)_{3-n}^{2+}$ family contrasting results have been reported: Cocks et al.[30] found dual emission from Ru → pq and Ru → bpy CT states, while Klassen[23] reports only emission from Ru → pq states. Figure 7 shows a schematic energy level diagram for $Ru(bpy)_3^{2+}$, $Ru(biq)_3^{2+}$, and $Ru(bpy)_2(biq)^{2+}$, where the information obtained from the temperature dependence results discussed below are also included.

Temperature Dependence. The ln $(1/\tau)$ vs. $1/T$ plots (Figures 4–6) have been obtained, with eq 1 and 2 fitted to the experimental points. As one can see from Table I, the k_0, A, and ΔE parameters are practically independent of the temperature range, showing that they concern intrinsic properties of the molecules.

The temperature dependence behavior of the $Ru(bpy)_3^{2+}$ emission lifetime is consistent with that described by other authors[5,13,24-26] in different or more limited temperature ranges, and/or different solvents. The most important features are (Table I, Figure 4) the presence of two[31] closely spaced ($\Delta E \approx 80$ cm^{-1}) states having similar decay properties and an excited state lying 4000 cm^{-1} above, which undergoes fast radiationless deactivation. The *increase* in the relative emission intensity upon increasing population of the excited state which lies 80 cm^{-1} above the lowest excited state is consistent with the results obtained by Hager and Crosby[13] on the luminescence behavior between 2 and 77 K, while the state lying ca. 4000 cm^{-1} above the lowest excited state[34] is the lowest triplet metal-centered (^{3}MC) excited state responsible for the photoracemization[32,33] and ligand photosubstitution[24,25] reactions.

For $Ru(biq)_3^{2+}$, temperature dependence experiments were carried out in both MeOH–EtOH and propionitrile–butyronitrile solvents because in the alcoholic solvent most of the ln $(1/\tau)$ vs. $1/T$ curve falls into the region of the glassy transition (Figure 6). For this complex very close-lying levels as for $Ru(bpy)_3^{2+}$ do not appear, probably because they are more tightly bunched. The very short-lived nonemitting level about 2700 cm^{-1} above the emitting Ru → biq triplet (Table I) is most likely the lowest ^{3}MC state,[34] which in $Ru(biq)_3^{2+}$ is expected to lie at much lower energy than in $Ru(bpy)_3^{2+}$ because the longer Ru–N bond distances,[35] caused by the steric hindrance among the biq ligands, strongly reduce the ligand field strength.

For $Ru(bpy)_2(biq)^{2+}$ (Figure 5, Table I, and Figure 7) very close lying levels do not appear, as in the case of $Ru(biq)_3^{2+}$. There is, however, a level at about 400 cm^{-1} above the emitting Ru → biq charge-transfer state which decays with $\tau = 1/A_1 \approx 50$ ns. Figure 5 also shows that the relative emission intensity does not decrease when this state is populated, indicating that such a state is another emitting Ru → biq CT excited state. Further increase in temperature (i.e., for $T >$ 250 K) causes a decrease in the emission intensity, suggesting that a nonemitting excited state begins to be populated. This last piece of information does not appear from the lifetime plot which only requires one exponential term in the temperature range explored.[36] According to the average ligand field rule,[37] the lowest ^{3}MC excited state of $Ru(bpy)_2(biq)^{2+}$ should lie 19 600 cm^{-1} above the ground state. It should also be noted that the steric hindrance caused by bpy on biq is much smaller than that caused by another biq, so that the biq contribution to the ligand field strength of $Ru(bpy)_2(biq)^{2+}$ may be larger than that evaluated from $Ru(biq)_3^{2+}$. Thus, the lowest ^{3}MC excited state of $Ru(biq)_3^{2+}$ may be closer to the lowest ^{3}MC of $Ru(bpy)_3^{2+}$ than the value estimated from the average ligand field. The level 400 cm^{-1} above the emitting excited state in $Ru(bpy)_2(biq)^{2+}$ can be neither a MC excited state (which is expected to occur above 19 600 cm^{-1}) nor a Ru → bpy CT excited state (which is expected to occur above 17 000 cm^{-1}). As previously mentioned, it can only be another Ru → biq charge-transfer excited state. The problem arises whether the splitting between the two low-lying Ru → biq CT excited states is due to different starting orbitals on the metal or different arriving orbitals on the ligand. In the latter case, the observed ΔE value would correspond to the splitting between the ψ and χ orbitals of biq. This, however, is implausible since, as previously mentioned, MO calculations of the EH type on the free ligand molecule yield a separation of 9000 cm^{-1}. Thus, the more likely explanation comes from symmetry considerations about starting orbitals on the metal. In the tris

(28) There is some controversy concerning the appropriateness of using spin labels.[4,6,14,15,17] Since this problem does not affect our discussion, we shall use spin labels for identification purposes.
(29) Anderson, S.; Seddon, K. R.; Wright, R. D.; Cocks, A. T. *Chem. Phys. Lett.* **1980**, *71*, 220.
(30) Cocks, A. T.; Wright, R. D.; Seddon, K. R. *Chem. Phys. Lett.* **1982**, *85*, 369.
(31) The results obtained by Hager and Crosby[13] between 2 and 77 K were interpreted on the basis of three closely spaced emitting levels (ΔE_1 = 10 cm^{-1}, ΔE_2 = 60 cm^{-1}). In the recent study by Durham et al.,[25] in the temperature range 230–300 K, fitting of the data required only one emitting level.
(32) Porter, G. B.; Sparks, R. H. *J. Photochem.* **1980**, *13*, 123. Hoggard, P. E.; Porter, G. B. *J. Am. Chem. Soc.* **1978**, *100*, 1457.
(33) Liebich, C. Diplomarbeit, University of Fribourg, Fribourg, Switzerland, 1980.
(34) Presumably this energy represents the barrier, rather than the minimum to minimum energy difference.
(35) Zehnder, M.; Belser, P.; von Zelewsky, A., presented at the 12th International Congress of Crystallography, Ottawa, Aug 1981, Abstract 09.4–40.
(36) Unfortunately boiling of the solvent prevents studies at higher temperature.
(37) Jørgensen, C. K. "Absorption Spectra and Chemical Bonding in Complexes"; Pergamon Press: London, 1962.

complexes a D_3 symmetry holds and the t_2 set of the $d(\pi)$ orbitals is split into $e(t_2)$ and $a_1(t_2)$ orbitals. CT states come from $e(t_2) \rightarrow a_2(\psi)$ and $e(t_2) \rightarrow e(\chi)$ orbital transitions and are of E symmetry.[15] In the $Ru(bpy)_2(biq)^{2+}$ case the trigonal symmetry lowers to digonal and the $e(t_2)$ orbitals of the metal t_2 set further split. The energy separation of 400 cm^{-1} could originate from splitting of the relevant E state. This interpretation would explain the lack of similar energy separation in $Ru(biq)_3^{2+}$, where trigonal symmetry is present.

Photochemical Implications. It has long been known that the $d(\pi) \rightarrow d(\sigma^*)$ MC excited states of d^6 octahedral complexes are inclined to undergo ligand dissociation.[38] A recent study by Durham et al.[25] has shown that this process is important for $Ru(bpy)_3^{2+}$ and that recoordination of the released bpy N atom reduces the quantum yield of photosubstitution products. Such a photodissociation reaction may be useful for preparative purposes, but it is harmful when $Ru(bpy)_3^{2+}$ is used as a photosensitizer. Our results (Table I, Figure 7) show that for $Ru(biq)_3^{2+}$ the photodissociative ^3MC excited state is easily populated at room temperature and it can be anticipated that this complex will undergo efficient photodissociation. By contrast, the lowest ^3MC excited state of $Ru(bpy)_2(biq)^{2+}$ is much less accessible because it is separated by about 5500 cm^{-1} from the lowest Ru $\rightarrow$ biq CT excited state (Figure 7). This suggests that $Ru(bpy)_2(biq)^{2+}$ could be less susceptible to photodissociation reactions. On the basis of the energy separation alone, one would also expect that $Ru(bpy)_2(biq)^{2+}$ is less susceptible to photodissociation than $Ru(bpy)_3^{2+}$. This would increase its interest as a photosensitizer for the water-splitting reaction.[20] For a definitive assessment of its stability toward irreversible photoreactions, the intrinsic reactivity of the ^3MC excited state has to be known, however.

Acknowledgment. This work was supported by the Italian National Research Council and Ministero della Pubblica Istruzione and by the Swiss National Science Foundation.

(38) Balzani, V.; Carassiti, V. "Photochemistry of Coordination Compounds"; Academic Press: London, 1970.

Contribution from the Department of Chemistry, Brooklyn Polytechnic Institute of New York, Brooklyn, New York 11201, Airtron, Inc., Morris Plains, New Jersey 07950, and the Department of Chemistry, The University of Mississippi, University, Mississippi 38677

Magnetic Properties of the Tetragonal Phase $K_xMn_xFe_{1-x}F_3$

E. BANKS,[†] M. SHONE,[‡] R. F. WILLIAMSON,[§] and W. O. J. BOO*[§]

Received March 3, 1983

The tetragonal tungsten bronze-like system $K_xMn^{II}_xFe^{III}_{1-x}F_3$ was studied at compositions $x = 0.40, 0.45, 0.50, 0.55$, and 0.60. Chemical composition and high precision lattice dimensions verify the composition span is $x = 0.40$–0.60. The interlayer distances of $K_xMn_xFe_{1-x}F_3$, including that of $KMnF_3$, obey the linear relationship $c' = 0.682 \log x + 4.182$. Structural constraints on antiferromagnetic ordering result in canted spin arrangements that, in turn, give rise to parasitic ferromagnetic moments. The values of T_N for $x = 0.40, 0.45, 0.50, 0.55$, and 0.60 are 162, 154, 148, 139, and 130 K, respectively, which are 0.6 times the predicted T_N values if no constraints were present. The values of C_M and Θ decrease dramatically as x increases, which is a consequence of a decreased number of nearest-neighboring Fe^{3+} ions. This further supports the supposition that $K_xMn_xFe_{1-x}Fe_3$ is ionically ordered over its entire composition span.

Introduction

The crystal structure determination of $K_{0.54}Mn_{0.54}Fe_{0.46}Fe_3$ [space group $P4_2bc$ (C^8_{4v})] by Banks, Nakajima, and Williams[1] established the existence of M^{2+}–M^{3+} ionic ordering in this phase. Ordering of this type may not be universal in fluoride analogues of tetragonal tungsten bronze, nor may it exist over the entire theoretical composition range ($0.4 \leq x \leq 0.6$); however, from their magnetic properties, it is likely that this same ionic ordering pattern exists in $K_xV^{II}_xV^{III}_{1-x}F_3$[2,3] and $K_xMn^{II}_xCr^{III}_{1-x}F_3$.[4]

The phase $K_xMn_xFe_{1-x}F_3$ can be thought of as x mol of $KMnF_3$[5] (perovskite) combined with $1 - x$ mol of FeF_3[6] (distorted ReO_3). All three of the structures are perovskite-like. Octahedra are corner sharing with M–F–M bond angles approximately 180°. Another property shared by these three compounds is their cations (Mn^{2+} and Fe^{3+}) have the same electronic configuration (d^5). In the octahedral crystal field provided by fluoride ions, orbital magnetic moments should be totally quenched, making these magnetic systems "spin only". Both $KMnF_3$ ($T_N = 88$ K)[7] and FeF_3 ($T_N = 394$ K)[8] order antiferromagnetically, and one would expect $K_xMn_xFe_{1-x}Fe_3$ to demonstrate the same behavior.

One feature that sets the bronze structure apart from the other two is that it contains structural constraints on antiferromagnetic ordering. These constraints are a consequence of two nearest-neighboring magnetic ions having a common nearest neighbor, making it impossible for magnetic moments on all nearest neighbors to be ordered antiparallel. In the bronze structure, there are four constraints per every 10 magnetic cations. Figure 1, which illustrates M^{2+}–M^{3+} ionic ordering in $K_{0.50}Mn_{0.50}Fe_{0.50}F_3$, also shows one of the four constraints (solid circle). One possible consequence of this kind of constraint is that in the magnetically ordered state, spins are forced to be canted. This may give rise to a small spontaneous magnetic moment (parasitic ferromagnetism).

Another consequence of magnetic constraints is to lower the ordering temperature T_N. If in the triangular arrangement,

[†] Brooklyn Polytechnic Institute of New York.
[‡] Airtron, Inc.
[§] The University of Mississippi.

(1) Banks, E.; Nakajima, S.; Williams, G. J. B. *Acta Crystallogr., Sect. B* **1979**, *B35*, 46.
(2) Williamson, R. F.; Boo, W. O. J. *Inorg. Chem.* **1977**, *16*, 649.
(3) Hong, Y. S.; Williamson, R. F.; Boo, W. O. J. *Inorg. Chem.* **1980**, *19*, 2229.
(4) Banks, E.; Shone, M.; Hong, Y. S.; Williamson, R. F.; Boo, W. O. J. *Inorg. Chem.* **1982**, *21*, 3894.
(5) Knox, K. *Acta Crystallogr.* **1961**, *14*, 583.
(6) dePape, R. *C. R. Hebd. Seances Acad. Sci.* **1965**, *260*, 4527.
(7) Hirakawa, K.; Hirakawa, K.; Hashimoto, T. *J. Phys. Soc. Jpn.* **1960**, *15*, 2063.
(8) Bacon, D. *Usp. Fiz. Nauk* **1963**, *8*, 335.

0020-1669/83/1322-3339$01.50/0